J|A|C|S
ARTICLES
Published on Web 03/08/2002

Heme Distortions in Sperm-Whale Carbonmonoxy Myoglobin: Correlations between Rotational Strengths and Heme Distortions in MD-Generated Structures

Christoph Kiefl,[†] Narasimha Sreerama,[†] Raid Haddad,[‡] Lisong Sun,[‡] Walter Jentzen,[‡] Yi Lu,[‡] Yan Qiu,[‡] John A. Shelnutt,*[,‡] and Robert W. Woody*[,†]

Contribution from the Department of Biochemistry and Molecular Biology, Colorado State University, Fort Collins, Colorado 80523, and Biomolecular Materials and Interfaces Department, Sandia National Laboratories, Albuquerque, New Mexico 87185-1349, and Department of Chemistry, The University of New Mexico, Albuquerque, New Mexico 87131

Received August 13, 2001. Revised Manuscript Received December 26, 2001

Abstract: We have investigated the effects of heme rotational isomerism in sperm-whale carbonmonoxy-myoglobin using computational techniques. Several molecular dynamics simulations have been performed for the two rotational isomers A and B, which are related by a 180° rotation around the $\alpha-\gamma$ axis of the heme, of sperm-whale carbonmonoxy myoglobin in water. Both neutron diffraction and NMR structures were used as starting structures. In the absence of an experimental structure, the structure of isomer B was generated by rotating the heme in the structure of isomer A. Distortions of the heme from planarity were characterized by normal coordinate structural decomposition and by the angle of twist of the pyrrole rings from the heme plane. The heme distortions of the neutron diffraction structure were conserved in the MD trajectories, but in the NMR-based trajectories, where the heme distortions are less well defined, they differ from the original heme deformations. The protein matrix induced similar distortions on the hemes in orientations A and B. Our results suggest that the binding site prefers a particular macrocycle conformation, and a 180° rotation of the heme does not significantly alter the protein's preference for this conformation. The intrinsic rotational strengths of the two Soret transitions, separated according to their polarization in the heme plane, show strong correlations with the ruffling deformation and the average twist angle of the pyrrole rings. The total rotational strength, which includes contributions from the chromophores in the protein, shows a weaker correlation with heme distortions.

Introduction

Heme b (protoheme IX) in hemoproteins can exist in two different orientations[1] that differ by a 180° rotation of the heme group about the $\alpha-\gamma$ axis (Figure 1), and the two rotational isomers are called isomers A and B. For isomer A, the porphyrin substituents as conventionally numbered (Figure 1) are arranged in a clockwise sense when viewed from the side of the proximal His for globins and other hemoproteins with a single protein ligand, or the N-terminal ligand for bis-liganded hemoproteins (e.g., cytochrome b_5). For isomer B, the porphyrin substituents are arranged in a counterclockwise sense. Twofold rotation about the $\alpha-\gamma$ axis interchanges the 2- and 4-vinyl groups with the 3- and 1-methyl groups, respectively, and leads to different protein−heme contacts. NMR studies have shown that the equilibrium ratio of A to B form depends on the protein sequence, and on the oxidation state and the ligands of the heme.[1] In sperm-whale myoglobin, isomer A is the predominant form. It has been shown that heme distortions can modulate physiologically important properties of hemoproteins.[2] Heme rotational isomerism could influence these physiologically important properties. Since the protein matrix can induce different distortions in isomers A and B, the heme in isomer B may exhibit different functional properties than that in isomer A.

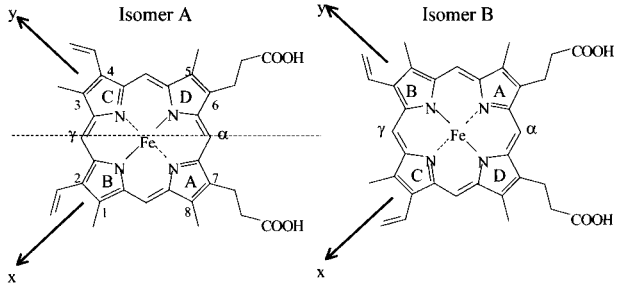

Figure 1. Isomers A and B, which differ by a 180° rotation of the heme about the $\alpha-\gamma$ axis in the protein matrix. This isomerization exchanges the position of the 2-vinyl with the 3-methyl and the 4-vinyl with the 1-methyl group. Vinyl groups are depicted in the *syn*-orientation. The pyrrole rings are identified by letters A to D, and the methine carbons by Greek letters α to δ. The view is from the proximal side of the heme.

Experimental results initially suggested that isomer B of native sperm-whale myoglobin has a 10-fold higher affinity for O_2 than isomer A.[3] However, subsequent experiments did not

* Corresponding authors. Robert W. Woody: Phone:(970) 491-6214; Fax (970) 491-0494, e-mail: rww@lamar.colostate.edu. John A. Shelnutt: Phone (505) 272-7160; Fax (505) 272-7077, e-mail: jasheln@unm.edu.
[†] Colorado State University
[‡] Sandia National Laboratories and University of New Mexico.

(1) La Mar, G. N.; Toi, H.; Krishnamoorthi, R. *J. Am. Chem. Soc.* **1984**, *106*, 6395−6401.

show any significant differences in the O_2- and CO-binding of native and reconstituted sperm-whale or yellowfin-tuna myoglobin.[4−6] The differences found in the first experiment were probably due to unrecognized irreversible oxidation of a fraction of heme, which resulted in higher apparent binding constants for O_2.[4] The O_2 affinity is probably modulated mainly by steric and electronic effects depending on the peripheral substituents.[7,8] However, the Bohr effect in *Chironomus thummi thummi* hemoglobins is affected by the heme rotational equilibrium.[8] The major form (isomer A) shows a large Bohr effect, whereas the minor form (isomer B) exhibits little or no Bohr effect. The heme isomers of bovine cytochrome b_5 have also been shown to differ in a physiologically relevant parameter: isomer A has a reduction potential that is 27 mV more negative than that of isomer B.[9]

Native sperm-whale myoglobin exhibits heme isomerism, with ∼10% of isomer B at equilibrium. Many high-resolution crystal structures have been reported for myoglobin, but only the A isomer has been observed in crystal structures[10] and NMR structures.[11] Freshly reconstituted myoglobin consists of a 50:50 mixture of the two isomers and reaches equilibrium at a rate that depends on several factors, such as species, pH, temperature, etc.[1] The Soret CD spectrum of freshly reconstituted myoglobin is only half as intense as that of the native protein, suggesting that isomer B has a weak, or even negative, Soret CD.[5,12] Extrapolation of the linear relation between the Soret CD intensity and the isomeric composition of the reconstituted carbonmonoxy myoglobin, as measured by NMR, gave a $\Delta\epsilon_{max}$ of +90 and −7 M^{-1} cm^{-1} respectively for isomers A and B.[13]

To examine the origins of differences in the Soret CD of the two isomers of myoglobin, we have performed MD simulations of sperm-whale myoglobin in both A and B forms. The structure of the B isomer, which is not available experimentally, was generated from the structure of isomer A by rotating the heme about the $\alpha-\gamma$ axis in the heme pocket. The calculated Soret CD spectra of the two isomers are qualitatively similar.

The origins of the Soret CD lie in the distortions of the heme, leading to an intrinsic rotational strength, and the interaction between the heme chromophore and the chromophores of the protein matrix.[14] In this paper we present the analysis of the protein-induced distortions of the heme in the MD trajectories for isomers A and B using normal-coordinate structural decomposition[15,16] (NSD) and another simple measure of heme distortion. We correlate the heme deformations with the calculated rotational strengths. The ruffling deformation[16] and the average twist angle of the opposite pyrrole rings, which also measures the ruffling deformation, show a strong correlation with the intrinsic rotational strengths of the two Soret transitions of the heme. The total rotational strength, which includes coupling with other chromophores in the protein, shows a weak correlation. A preliminary account of this work was presented at an Alcuin Symposium.[17]

Methods

MD-Simulation. Molecular dynamics simulations of the two rotational isomers of sperm-whale carbonmonoxy myoglobin in water have been performed at 300 K with GROMOS96.[18] The starting structures of the protein were taken from a neutron-diffraction structure[10] (PDB entry 2mb5) and two of twelve NMR structures[11] (PDB entry 1myf). After placing the protein in a rectangular box of equilibrated extended simple-point-charge (SPC/E) water[19] molecules and removing water molecules within a 2.3 Å radius of any non-hydrogen protein atoms, two cycles of steepest-descent energy minimization were performed. In the first cycle, the positions of the protein atoms were restrained, but in the second, no restraints were applied. All covalent bond lengths and the H_2O bond angle in this and subsequent steps were constrained to their equilibrium values with SHAKE,[20] with a geometric tolerance of 10^{-4}. Eight water molecules were replaced by Cl^- ions to maintain electroneutrality, followed by two cycles of steepest-descent energy minimization, as described above. This was followed by 20 steps of conjugate-gradient energy minimization. The molecular dynamics simulation under periodic boundary conditions was then initiated, starting at 100 K, and using an integration time step of 2 fs. Three steps followed, each of 5 ps duration, in which the temperature was increased by 100 K per step, and restraints were decreased. Three more steps, each of 5 ps duration, followed at 100, 200, and 300 K, without restraints. Finally, unrestrained simulation at 300 K for 20 ps completed the equilibration process. Nonbonded interactions were calculated with a triple-range method,[21] with cutoffs of 8 and 14 Å. Coordinates were saved at 0.050-ps intervals. Further details are provided in the Supporting Information.

We performed four MD simulations for each isomer, with four different initial velocity assignments, using the neutron-diffraction structure[10] as the starting geometry. The starting geometry for isomer B was obtained from the isomer A structure by rotation of the heme by 180° about the $\alpha-\gamma$ axis, keeping the vinyl groups in plane and in the syn conformation, as shown in Figure 1. The four MD trajectories of isomer A, generated with the neutron-diffraction structure and different initial velocities, are referred to as T1A, T2A, T3A, and T4A. The corresponding trajectories of isomer B are referred to as T1B−T4B. We have also performed MD simulations with two starting structures taken from the ensemble of twelve NMR structures,[11] structures #1 (1myf-1) and #8 (1myf-8), and these MD trajectories are referred to as N1 and N2, respectively, with the isomer indicated by A and B, e.g., N1A for isomer A with NMR structure #1 as the starting geometry. These MD simulations were performed on two of the original

(2) Shelnutt, J. A.; Song, X. Z.; Ma, J. G.; Jia, S. L.; Jentzen, W.; Medforth, C. J. *Chem. Soc. Rev.* **1998**, *27*, 31−41.
(3) Livingston, D. J.; Davis, N. L.; La Mar, G. N.; Brown, W. D. *J. Am. Chem. Soc.* **1984**, *106*, 3025−3026.
(4) Aojula, H. S.; Wilson, M. T.; Morrison, I. E. G. *Biochem. J.* **1987**, *243*, 205−210.
(5) Light, W. R.; Rohlfs, R. J.; Palmer, G.; Olson, J. S. *J. Biol. Chem.* **1987**, *262*, 46−52.
(6) Neya, K.; Funasaki, N.; Shiro, Y.; Iizuka, T.; Imai, K. *Biochim. Biophys. Acta* **1994**, *1208*, 31−37.
(7) Chang, C. K.; Ward, B.; Ebina, S. *Arch. Biochem. Biophys.* **1984**, *231*, 366−371.
(8) Gersonde, K.; Sick, H.; Overkamp, M.; Smith, K. M.; Parish, D. W. *Eur. J. Biochem.* **1986**, *157*, 393−404.
(9) Walker, F. A.; Emrick, D.; Rivera, J. E.; Hanquet, B. J.; Buttlaire, D. H. *J. Am. Chem. Soc.* **1988**, *110*, 6234−6240.
(10) Cheng, X.; Schoenborn, B. P. *J. Mol. Biol.* **1991**, *220*, 381−399.
(11) Osapay, K.; Theriault, Y.; Wright, P. E.; Case, D. *J. Mol. Biol.* **1994**, *244*, 183−197.
(12) Aojula, H. S.; Wilson, M. T.; Drake, A. *Biochem. J.* **1986**, *237*, 613−616.
(13) Aojula, H. S.; Wilson, M. T.; Moore, G. R.; Williamson, D. J. *Biochem. J.* **1988**, *250*, 853−858.
(14) Hsu, M. C.; Woody, R. W. *J. Am. Chem. Soc.* **1971**, *93*, 3515−3525.
(15) Jentzen, W.; Ma, J. G.; Shelnutt, J. A. *Biophys. J.* **1998**, *74*, 753−763.
(16) Jentzen, W.; Song, X. Z.; Shelnutt, J. A. *J. Phys. Chem. B* **1997**, *101*, 1684−1699.
(17) Woody, R. W.; Kiefl, C.; Sreerama, N.; Lu, Y.; Qiu, Y.; Shelnutt, J. A. In *Insulin and Related Proteins: From Structure to Function and Pharmacology*; Federwisch, M., Dieken, M. L., Eds.; Kluwer Academic Publishers: Dordrecht, The Netherlands, 2002 (in press).
(18) van Gunsteren, W. F.; Billeter, S. R.; Eising, A. A.; Hünenberger, P. H.; Krüger, P.; Mark, A. E.; Scott, W. R. R.; Tironi, I. G. *Biomolecular Simulations: The GROMOS96 Manual and User Guide*; Hochschulverlag AG an der ETH: Zürich, 1996.
(19) Berendsen, H. J. C.; Grigera, J. R.; Straatsma, T. P. *J. Phys. Chem.* **1987**, *91*, 6269−6271.
(20) Ryckaert, J. P.; Ciccotti, G.; Berendsen, H. J. C. *J. Comput. Phys.* **1977**, *23*, 327−341.
(21) van Gunsteren, W. F.; Berendsen, H. J. C. *Angew. Chem., Int. Ed. Engl.* **1990**, *29*, 992−1023.

NMR structures instead of using the average of the twelve NMR structures. In this way, we covered more conformational space and additionally could monitor the dependence of MD-generated structures on initial distortions. The trajectories N1 and N2 have different starting geometries, whereas trajectories T1 to T4 have the same starting geometry but differ in their initial velocities.

For comparison with the myoglobin MD simulations, a 600-ps MD simulation of Fe(III) protoporphyrin chloride (FePP(Cl)) was performed by using the POLYGRAPH 3.21 program and a DREIDING II force field (MSI) modified to include atom types for the heme with fractional atomic charges as previously described.[2,16] The MD calculation was run by using canonical NVT dynamics at 300 K while saving snapshot structures at 0.05-ps intervals. The snapshots from the FePP(Cl) MD trajectory were analyzed in terms of the normal coordinate deformations in the same way as the myoglobin MD trajectories.

Intrinsic Rotational Strength. Circular dichroism ($\Delta\epsilon$) is the differential absorption of left and right circularly polarized light,

$$\Delta\epsilon = \epsilon_L - \epsilon_R \tag{1}$$

where ϵ_L and ϵ_R are respectively the molar decadic extinction coefficients for left- and right-circularly polarized light. The rotational strength of a transition from the ground state *0* to excited state *a* is determined by integrating the intensity under a single band in the CD spectrum, according to:

$$R_{0a} = (3000\hbar c \ln 10/16\pi^2 N_A) \int_{\text{band}} (\Delta\epsilon/\lambda)\, d\lambda = 0.2477 \int_{\text{band}} (\Delta\epsilon/\lambda)\, d\lambda \tag{2}$$

where $\hbar$ is Planck's constant divided by 2π, c is the velocity of light, and N_A is Avogadro's number. Rotational strength is usually expressed in Debye−Bohr magnetons (1 DBM = 0.9273×10^{-38} cgs units). The numerical factor in the second form of eq 2 provides R in DBM when $\Delta\epsilon$ is in M^{-1} cm^{-1}.

The rotational strength can be calculated theoretically[22] from the imaginary part of the scalar product of the electric and magnetic dipole transition moments:

$$R_{0a} = \text{Im}\{(0|\mu|a)\cdot(a|\mathbf{m}|0)\} \tag{3}$$

where μ is the electric dipole transition moment operator, a measure of the linear displacement of charge upon excitation; and **m** is the magnetic dipole transition moment operator, a measure of the circular displacement of electron density upon excitation. The superposition of μ and **m** results in a helical displacement of charge, which interacts differently with left- and right-circularly polarized light.

There are two types of contributions to the rotational strengths of the two Soret components: the intrinsic rotational strength of the transitions resulting from the inherent chirality of the heme, and the perturbations resulting from coupling of the heme transitions with transitions in other chromophores in the protein, of which the aromatic side chains and the backbone peptide groups are the most important. In this paper, we consider only the intrinsic rotational strengths of the Soret components. The extrinsic contributions arising from coupling of these transitions to proteins groups are treated in another paper (Kiefl et al., in preparation).

The intrinsic rotational strengths for the Soret components were calculated according to the equation:

$$R_{0a} = -(e^2\hbar^2/4\pi m^2 c\nu_{0a})(0|\nabla|a)\cdot(a|r \times \nabla|0) \tag{4}$$

where $(0|\nabla|a)$ is the dipole velocity matrix element connecting the ground state, *0*, and the excited state, *a*; $(a|r \times \nabla|0)$ is a matrix element connecting the ground state, *0*, and the excited state, *a*, that is proportional to the angular momentum of the transition $0 \rightarrow a$; ν_{0a} is the frequency (s^{-1}) of the transition $0 \rightarrow a$; and e and m are respectively the charge and mass of the electron. This formulation of the rotational strength, known as the dipole velocity form, is origin-independent,[23] in contrast to the dipole length form in eq 3.

In these calculations we treated the heme as a porphyrin dianion, considering only the π electrons, neglecting the methyl and propionyl side chains, but including the two vinyl groups. The π-system in the heme group contained 28 atoms. The transition parameters and intrinsic rotational strength of the Soret transitions were calculated by using π-molecular orbital theory in the Pariser−Parr−Pople (PPP) approximation[24] with parameters from the "standard model" of Weiss et al.[25] The calculations were performed on the heme structures in the MD trajectories at 0.05-ps intervals. In this paper, we will only consider the intrinsic rotational strengths of the heme. The total rotational strengths of the heme transitions, including contributions of coupling with transitions in protein chromophores, are described elsewhere (Kiefl et al., in preparation).

The Soret CD band has two nearly degenerate components that are polarized in the plane of the heme and perpendicular to each other. The near-degeneracy of the Soret components leads to fluctuations in the relative energies of the *x*- and *y*-polarized Soret components, precluding a unique correlation using the energy classification. The two Soret components were distinguished according to their polarization in the heme-plane, which gives a good correlation with a measure of heme distortion as described below. Each Soret transition moment was assigned as either *x*- or *y*-polarized, according to the angle of its projection on the mean plane of the heme, using ±45° lines as boundaries. The *x*-axis passes through the nitrogen atoms of the pyrroles D and B (N_D- - -N_B) and the *y*-axis through A and C pyrroles (N_A- - -N_C) (Figure 1). The calculated rotational strengths for the *x*- and *y*-polarized components were separately averaged over the trajectory.

Normal-Coordinate Structural Analysis. Heme structures were analyzed by normal-coordinate structural decomposition (NSD) as described earlier.[15,16] Figure 2 illustrates the NSD method for the heme from the X-ray crystal structure of horse heart cytochrome *c*. The computational procedure projects out the deformations along all of the 66 normal coordinates of the porphyrin macrocycle, including both in-plane and out-of-plane modes. Typically for hemoprotein crystal and NMR structures, however, the deformations are only large enough to be statistically significant for the lowest frequency out-of-plane modes. This is because these modes have the smallest restoring forces and thus tend to have the largest deformations from planarity. For porphyrin crystal structures, which are usually refined to much higher resolution than hemoproteins, the lowest frequency modes alone do not provide a sufficient description of the structure,[15] but for the hemoproteins, a description in terms of the deformations of only the lowest frequency normal modes is adequate statistically. That is, the error in the structure when the contributions from all of the other modes are neglected is less than the positional uncertainty in the X-ray structure.

For this work, a C version of the NSD program was modified for input of the 12 000 snapshot structures from the MD simulation. Time-averaged plots were obtained by using the 2D smoothing function of SigmaPlot2001, which uses a Gaussian weighting function over a 6-ps sliding window and a linear fitting function. The fast Fourier transform of the POWSPEC program of SigmaPlot was applied to the deformations in the first 8192 (2^{13}) structures of the trajectories T2A, T2B, and FePP(Cl). Deformations along each of the normal modes were weighted by a cosine function that vanishes at the endpoints of the data (Hanning window[26]), thus removing high-frequency components generated by using a finite trajectory. The magnitudes resulting from

(22) Rosenfeld, L. *Z. Phys.* **1928**, *52*, 161−174.

(23) Moffitt, W. *J. Chem. Phys.* **1956**, *25*, 467−478.
(24) (a) Pariser, R.; Parr, R. G. *J. Chem. Phys.* **1953**, *21*, 466−471; 767−776. (b) Pople, J. A. *Trans. Faraday Soc.* **1953**, *49*, 1375−1385.
(25) Weiss, C.; Kobayashi, H.; Gouterman, M. *J. Mol. Spectrosc.* **1965**, *16*, 415−450.

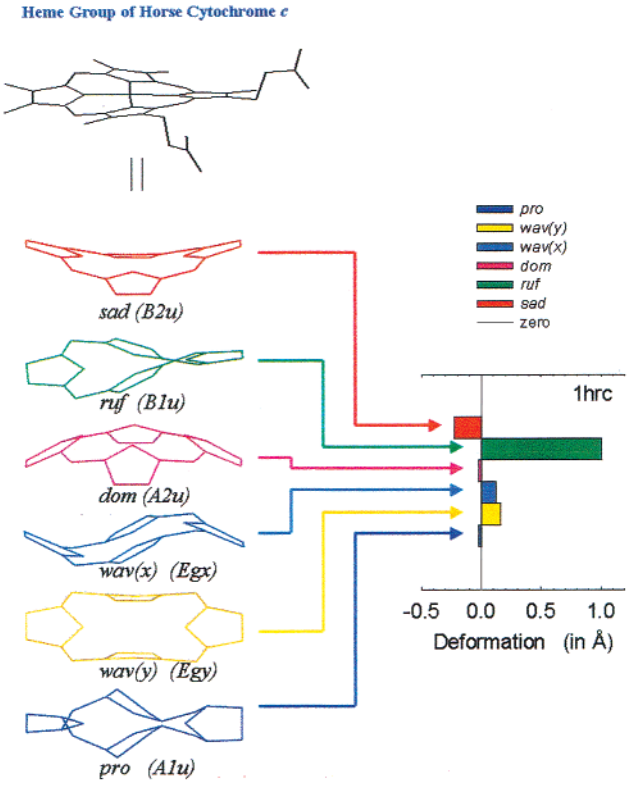

Figure 2. Illustration of the heme distortions characterized by normal-coordinate structural decomposition of the heme from horse heart cytochrome *c*. The distorted structure at the top left is that of the heme in horse-heart cytochrome *c*. Each of the six structures below it shows the heme deformed along one of the lowest-frequency normal modes. Each deformation belongs to an irreducible representation of the D_{4h} symmetry group appropriate to the planar, 4-fold symmetric porphyrin nucleus. A linear combination of these deformations, called saddling (*sad*), ruffling (*ruf*), doming (*dom*), waving-*x* (*wavx*), waving-*y* (*wavy*), and propellering (*pro*), can be fit to an arbitrarily deformed heme within the experimental error of protein crystal structures. The coefficients in the linear combination required to fit horse-heart cytochrome *c* are represented in the bar plot on the right. These coefficients are the displacements in Å along these six normal coordinates that best represent the out-of-plane distortion of the heme structure.

the transform were squared and multiplied by two to yield the power spectral density as a function of frequency.

Twist-Angle (τ). The virtual dihedral angles between the two sets of opposing pyrrole rings can be used to characterize the overall distortion of the heme. These relate the pyrrole rings A↔C and B↔D (see Figure 1) and are denoted τ_{AC} and τ_{BD}, respectively. The dihedral angle τ_{AC} is determined by sighting along the line connecting the midpoints of pyrroles A and C. The angle carrying the $C_{2B}-C_{3B}$ bond of pyrrole A into the $C_{4B}-C_{5B}$ bond of pyrrole C is τ_{AC}. An analogous procedure is used to define τ_{BD}. A planar heme has both τ_{AC} and τ_{BD} equal to 0°. These two dihedral angles give a measure of the twist of the pyrrole rings with respect to the heme plane and are inversely related. Generally, a positive AC twist ($0° < \tau_{AC} < 90°$) is compensated by a negative BD twist ($-90° < \tau_{AC} < 0°$), which is a consequence of the constraints of the heme macrocycle. For small values of τ_{AC} and τ_{BD}, the inverse relation may not be satisfied, but the heme deformations are also small in such cases.

The average twist angle (τ) was calculated by averaging the absolute values of the two dihedral angles and retaining the sign of the AC twist angle. The average twist angle shows a strong correlation with the ruffling deformation from the NSD analysis. The propellering deformation also gives rise to opposite signs of τ_{AC} and τ_{BD}, but the average propellering deformation is much smaller than the ruffling deformation.

Results and Discussion

Heme Distortions: Normal Coordinate Structural Analysis. The major heme deformations that make up the distortion in hemoproteins are *ruffling* (*ruf*), *saddling* (*sad*), and *doming* (*dom*), whereas *waving* (*wav*(*x*), *wav*(*y*)) and *propellering* (*pro*) deformations tend to be smaller due to their higher vibrational frequencies[15,16] (Figure 2). These six macrocycle deformations are unique because they correspond to the lowest frequency out-of-plane vibrational modes of B_{1u}, B_{2u}, A_{2u}, E_g, and A_{1u} symmetries (irreducible representations), respectively, of the nominal D_{4h} molecular symmetry of hemes. Using NSD, the out-of-plane distortion of most heme structures can be well represented in terms of the normal coordinate displacements for these six vibrational modes.

The out-of-plane heme distortions in myoglobin are generally small in comparison with other hemoproteins.[15] For the 14 experimental structures of sperm-whale carbonmonoxy-myoglobin obtained by X-ray diffraction (1vxf), neutron diffraction (2mb5), and NMR spectroscopy (1myf: 12 structures), the total out-of-plane distortions are generally less than 0.7 Å. The consistent features of the experimental heme structures from all sources are the small, positive doming, *y*-waving, and propellering deformations (<0.5 Å). All other deformations are also small (<0.4 Å) and can be either positive or negative, but the *wav*(*x*) deformation is typically negative. These features are quite general for myoglobins, as shown by an NSD analysis of 99 crystal structures of Fe(III) myoglobin derivatives, especially the *wav*(*y*) deformation (Supporting Information).

The NSD results for the 600-ps averaged structures show that deformations of all crystal-based trajectory structures are largely conserved for isomers A and B and differ only in their amplitudes (Figure 3). This is probably because the trajectories have the same starting structure and differ only in their initial velocities. Further, at least the signs of the initial deformations of the neutron-diffraction heme structure are conserved in all of the averaged structures of the crystal-based trajectories for isomer A, except for *dom* in T3A. However, the 600-ps averaged heme distortions in trajectories N1A and N2A (Figure 3) are very different from the original heme distortions of NMR structures 1myf-1 and 1myf-8, respectively. This may reflect the fact that heme distortions are not completely characterized by NMR signals, i.e., only the outer C-atoms of the heme are well characterized, whereas the positions of the inner C-atoms of the macrocycle are due to the force field used in the NMR structure determination.

The NSD results show that there are clear differences between the neutron-diffraction (crystal) and NMR-based (solution) heme distortions due to the different starting structures (Figure 3). For the 600-ps averaged heme structures, the distortions in isomer A for the crystal-based trajectories are mostly dominated by positive saddling, ruffling, *y*-waving, and propellering. The deformations in isomer A for the NMR-based trajectories have the same sign, except for ruffling (in trajectories N1A and N2A) and propellering (in trajectory N1A), which are negative. In isomer B, ruffling and saddling dominate the deformations for the crystal-based trajectories: saddling, *y*-waving, and propellering are positive, and ruffling, doming, and *x*-waving are

(26) Press, W. H.; Flannery, B. P.; Teukolsky, S. A.; Vetterling, W. T. *Numerical Recipes: The Art of Scientific Computing*; Cambridge University Press: Cambridge UK, 1989; p 425.

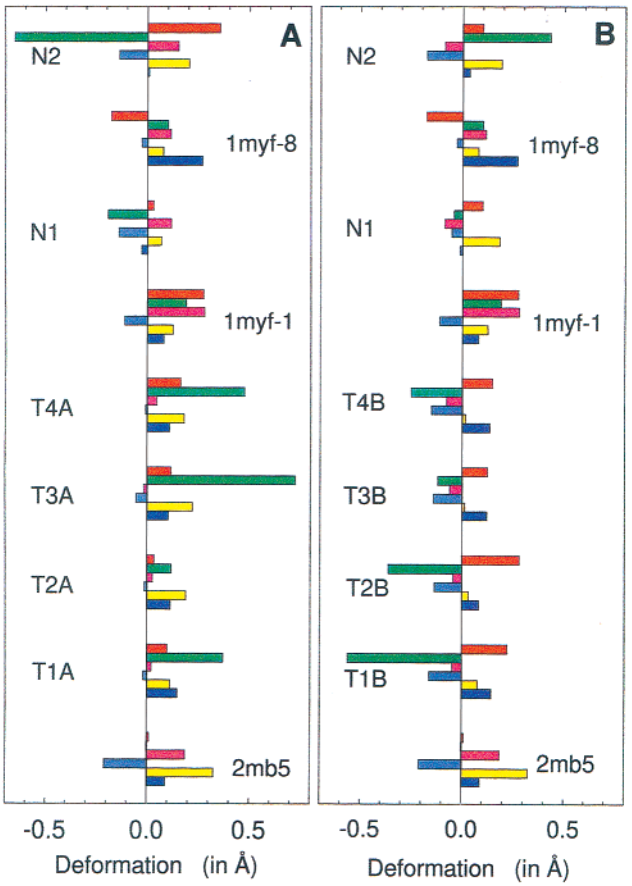

Figure 3. Out-of-plane deformations of the heme in the starting structures and in the 600-ps averages over the MD trajectories for NMR- and crystal-based calculations for isomer A (left) and isomer B (right). The trajectories T1 to T4 are based on the neutron diffraction structure 2mb5 and differ only in their initial velocities. The trajectories N1 and N2 are based on the NMR solution structures 1myf-1 and 1myf-8, respectively, and differ in their starting geometries. The deformations are in the order *sad*, *ruf*, *dom*, *wav(x)*, *wav(y)*, and *pro*, and the color coding is as shown in Figure 2.

negative. These signs are again conserved in isomer B, for N1B and N2B, except for ruffling in trajectory N2B.

The comparison of the heme deformations between isomers A and B requires a careful examination. At first sight, there seems to be a clear difference between A and B in all trajectories, but we have to consider the symmetry operations due to the heme rotation (see relationships below). To see the effects of the rotation, we must first understand the way in which the NSD analysis of heme structures is done and the resulting sign convention for the individual deformations. All hemes are analyzed by first orienting the heme as shown in Figure 1 (isomer A). The asymmetric substitution pattern of protoporphyrin IX allows the heme to be uniquely positioned and thus the heme conformation to be uniquely expressed by the NSD-determined normal-coordinate displacements. The uniqueness in the orientation used for NSD leads to the unique sign convention for protoporphyrin IX deformations. Now consider a purely ruffled heme structure. In the *ruf* deformation, the pyrrole rings are twisted about the metal−nitrogen bonds (Figure 2). This twist can occur in a positive or negative sense relative to the mean plane of the heme. For symmetrically substituted hemes, there would be ambiguity in the absolute sign of the ruffling because there is no unique way to orient the heme for the NSD analysis, e.g., the macrocycle could be rotated by 90° about the *z*-axis or rotated about an in-plane symmetry axis, reversing the sign of the ruffling. For asymmetrically substituted hemes such as protoheme, the sign convention is determined because we always orient the heme as shown for isomer A in Figure 1, prior to the NSD analysis.

Now consider the scenario in which the heme is rotated by 180° about the α−γ axis within the specific protein environment of myoglobin. For simplicity, assume that the protein imposes exactly the same distortion on the macrocycle of the rotated heme. Then detailed considerations described below show that the NSD deformations transform as follows:

$$ruf \rightarrow -ruf$$

$$sad \rightarrow sad$$

$$dom \rightarrow -dom$$

$$wav(x) \rightarrow -wav(y)$$

$$wav(y) \rightarrow -wav(x)$$

$$pro \rightarrow pro$$

As an example of how these relationships are determined, consider a heme-binding site that favors a purely ruffled macrocyclic structure in which the α and γ positions are above the mean plane and the β and δ positions are below the plane. If the heme is rotated 180° about the α−γ axis and the heme structure is unchanged, then the α- and γ-carbons are now below the mean plane. This does not change the NSD results, because the heme would be rotated back to the orientation shown in Figure 1 (isomer A) for analysis. However, if the heme site in the protein prefers the α and γ positions to be above the plane, the conformation of the rotated heme is changed. This rotated structure, with the α- and γ-carbons forced above the plane by the protein, must also be put back into the orientation in Figure 1 (isomer A) for the NSD analysis. However, when reoriented, the α and γ positions are now below the plane, thus changing the sign of the ruffling as indicated in the above relationship. Similar arguments apply for the other deformation types.

In light of the relationships associated with rotational isomerism in the heme site, the differences in structure of isomers A and B seen in the 600-ps averaged structures (Figure 3) make good sense qualitatively. Comparing isomers A and B in Figure 3, we see that ruffling and doming typically have opposite signs for A and B, in agreement with the expected relationships. Also as expected, the *sad* and *pro* deformations have the same signs for isomers A and B. Furthermore, if the magnitude of the *wav*(*x*) deformation is large and *wav*(*y*) is small for the B isomer, then *wav*(*y*) is large and *wav*(*x*) is small for the A isomer. This is consistent with the switching of *x* and *y* in the expected relationships. The relative signs of *wav*(*x*) and *wav*(*y*) do not usually differ between isomers A and B because these deformations usually have opposite signs for a heme structure. This ensures that the minus sign in the relationships for the wave deformation cancels with the relative sign between the deformations, so all we observe is the switching of the magnitudes. From these NSD results, we must conclude that the binding site prefers a particular macrocycle conformation, and that 180° rotation of the heme does not greatly alter the protein's preference for this conformation.

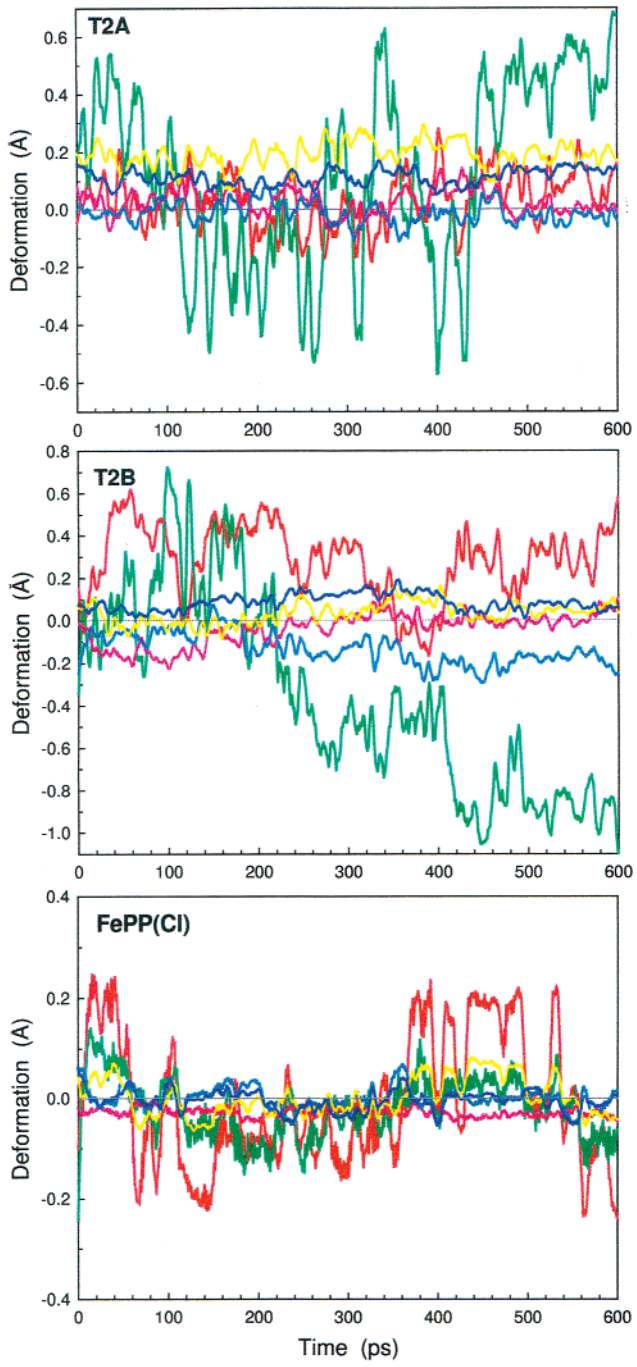

Figure 4. Out-of-plane deformations of the heme structures for the (a) T2A, (b) T2B, and (c) FePP(Cl) trajectories. The deformations are smoothed over a 6-ps interval, as described in the text, and are color-coded as shown in Figure 2.

Figure 4 illustrates the running average deformations over the 600-ps trajectories T2A, T2B, and FePP(Cl). The plots shown are obtained from a weighted average over 6-ps intervals. Clearly, the heme ruffling exhibits transient deformations of more than 0.5 Å that last for tens to hundreds of picoseconds. These drifts in an out-of-plane deformation may be part of nanosecond scale oscillations in the heme deformations, but longer MD simulations will be necessary to determine this. Doming and saddling show similar variations, but the amplitudes of the average motion are smaller than for the softer ruffling deformation. It is clear that much longer MD calculations are required to truly average over these variations in the macrocycle structure. For most of the deformations, the amplitude of vibration is larger than the offset in the equilibrium position, and thus the structures obtained by averaging over 6 ps of the trajectory represent the shifting of the equilibrium position about which the heme vibrates.

Deformations on the order of 1 Å are large enough to change physical properties of the heme such as redox potentials, Fe d-orbital populations, and spin state, and are likely able to affect biological properties as well.[2] The long time scale (>10 ps) of these out-of-plane deformations suggests that they may reflect large-scale motions of the protein structure or structural substates of the heme pocket that persist for long times. Detailed analyses of the motions of the amino acid side chains in the heme pocket will be required to test this hypothesis.

Some deformations of the heme of myoglobin are strongly maintained by the protein structure, *y*-waving, and propellering deformations in particular. While small, the average deformations are never negative and in fact show only small variations about the 600-ps average value.

The free heme shows much smaller short-time average deformations, which average to near zero over the entire 600-ps trajectory (Figure 4c). As for myoglobin, saddling and ruffling deformations show the largest transient excursions. For FePP(Cl) saddling seems to have the largest amplitude, but for myoglobin ruffling has the largest amplitude. The 6-ps averages indicate that the saddling, ruffling, and *y*-wave motions are correlated on these time scales. These motions may be associated with the flipping of the vinyl groups from side to side, which also occurs on 10- to 100-ps time scales.

When NSD is applied to each recorded structure (0.05-ps intervals), high-frequency oscillations of the deformations are observed. Figure 5 shows NSD results over 10 ps of an MD trajectory (T2A). Ruffling shows both the longest period of oscillation (~1 ps) and the largest amplitude. The period puts the frequency in the tens of cm^{-1} range, close to the expected vibrational frequency[15] of the normal mode corresponding to the ruffling vibration of the macrocycle. The regular sinusoidal vibrational motion is, however, altered by interaction with the changing protein environment, as well as other factors. For the other deformations, inspection of Figure 5 shows that the frequency increases and the amplitude decreases, as expected from values obtained from independent normal coordinate analyses of porphyrin motion. That is, the apparent frequencies increase in the order *ruf* < *sad* < *dom* ~ *wav*(*x*) ~ *wav*(*y*) < *pro*. This frequency order is obtained by Fourier transforms of time-domain data shown in Figure 4. The apparent amplitudes decrease in the same order.

The power spectra obtained from the Fourier transforms (Supporting Information) show that the order of frequencies agrees approximately with the order of the frequencies obtained in the normal coordinate calculations[16] from which the normal coordinate eigenvectors used in the NSD analysis are obtained. Exact agreement is not expected because the substituent masses are set to zero to obtain the eigenvectors of the bare macrocycle for the NSD basis vectors. For a substituted porphyrin like protoporphyrin IX, these macrocycle motions are mixed with the substituent and metal motions to give the normal coordinates of the protoheme IX. The mixing may account for the multiple peaks observed in the Fourier transforms.

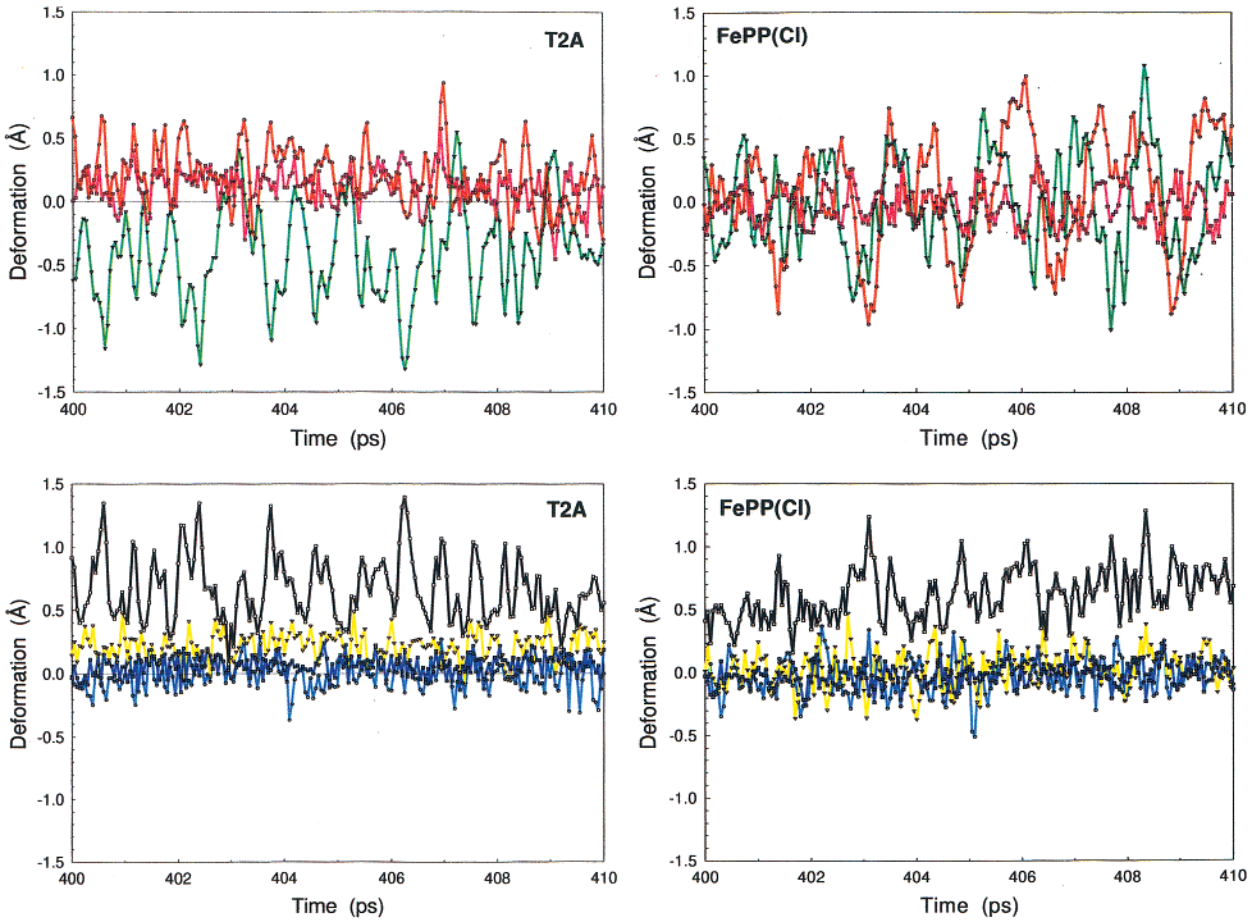

Figure 5. Time course of the individual out-of-plane deformations for MD simulations for isomer A of MbCO (trajectory T2A) and for FePP(Cl) over a 10-ps interval near the middle of 600-ps trajectories. The time courses are color-coded as in Figure 2. (a) *sad*, *ruf*, and *dom* deformations in trajectory T2A; (b) *wav(x)*, *wav(y)*, and *pro* deformation and the total distortion in trajectory T2A; (c) *sad*, *ruf*, and *dom* deformations in trajectory FePP(Cl); (d) *wav(x)*, *wav(y)*, and *pro* deformation and the total distortion in trajectory FePP(Cl).

The main difference between the isolated heme and the heme in myoglobin is the broadening of the peaks in the power spectrum of the protein-bound heme. This is probably brought about by the motion of the protein environment in which the heme sits. There is little difference between the A and B isomers in this regard. The peak frequencies of the heme of myoglobin are mirrored by the peaks of the isolated heme, indicating that neither the differences in force fields used in the calculations nor the presence of the protein matrix have a strong effect on the natural vibrational frequencies of the heme aside from the observed broadening and shifts in frequency distribution and intensity.

The average values of the *wav*(*y*) and *pro* deformations (approximately 0.2 and 0.1 Å, respectively) evident from the 400−410 ps trajectory shown in Figure 5 are in good agreement with the longer 6-ps averages (Figure 4) and the full 600-ps averaged structures (Figure 3) for this trajectory. The positive average value for the *ruf* deformation may also be evident to the eye from Figure 4a. It is important to note that such excursions in ruffling on a picosecond time scale are much larger than the average *ruf* deformation for the 600-ps trajectory and also the ruffling seen experimentally in crystal structures.[16]

Transient ruffling on the order of 1−2 Å is large enough to cause d-orbital configuration changes in hemes. Nakamura et al.[27] observed different d-orbital configurations for ruffled and planar low-spin Fe(III) porphyrins, demonstrating that ruffling can induce the $d_{\pi}^3,d_{xy}^2 \rightarrow d_{\pi},^4d_{xy}^1$ transition and thereby influence hemoprotein function. Our MD simulations suggest that even for hemoproteins such as myoglobin, which show only small static ruffling deformations, deformations of the order of 1 Å occur transiently on 10−100 ps time scales, and thus the d-orbital configuration may transiently change as well. In proteins such as the *c*-type cytochromes, for which the average structure is already ruffled by about 1 Å, even larger excursions in the ruffling may occur transiently. The associated effects on the d-orbital occupations could easily influence the electron-transfer function of cytochromes, possibly even providing an electron gating mechanism.

Heme Distortions: Twist Angle. The average twist angle τ can also be used to characterize the overall heme distortions. This angle represents the average twist of the pyrrole rings with respect to the plane of the heme macrocycle and is strongly correlated with the ruffling (*ruf* distortion) characterized from the NSD analysis. The strong correlation ($r = 0.99$) between these two measures of heme distortion for the T2A trajectory is shown in Figure 6. Ruffling is a major type of distortion in heme, shows the largest amplitudes and oscillations (Figure 5), and is particularly important in the CD calculations. The twist angle might appear to be redundant, given the excellent correlation with the *ruf* distortion. However, the twist angle can

(27) Nakamura, M.; Ikeue, T.; Fujii, H.; Yoshimura, T. *J. Am. Chem. Soc.* **1997**, *119*, 6284−6291.

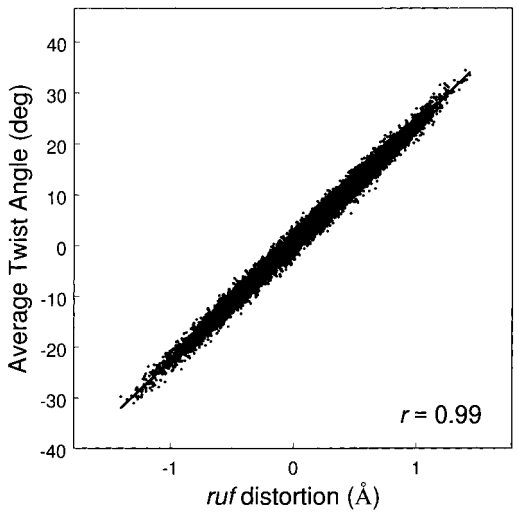

Figure 6. Correlation between the average twist angle (τ) and ruffling deformation (*ruf*) for the T2A trajectory.

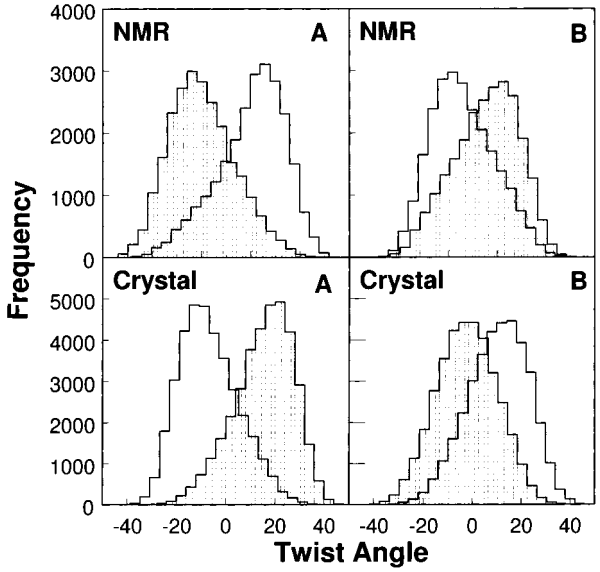

Figure 7. Distribution of the twist angles τ_{AC} (fill pattern: vertical bars) and τ_{BD} (fill pattern: squares) for the crystal- and NMR-based trajectories.

be calculated very easily and does not require the use of the full NSD analysis. Therefore, the twist angle is useful if one is primarily interested in correlating the heme conformation with intrinsic rotational strengths of the Soret transitions.

The distributions of the twist angles, τ_{AC} and τ_{BD}, for the crystal- and NMR-based simulations are shown in Figure 7. It is clearly evident from this distribution that the positive twist of one set of pyrroles is accompanied by a negative twist of the other set. The strain of the twist from one set of pyrroles, say A↔C, on the ring system of the heme macrocycle is relieved by twisting the second set of pyrroles (B↔D) in the opposite direction. The differences between the twist angle distributions in the two isomers is also evidenced in Figure 7. The two distributions are approximately interchanged between the two isomers. In isomer A, the τ_{AC} distribution spans negative values, while τ_{BD} spans positive values. The situation is reversed in isomer B, where τ_{BD} spans negative values and τ_{AC} spans positive values. The two isomers are related by a 180° rotation about the $\alpha-\gamma$ heme axis, which interchanges the pyrrole rings A and B, and C and D, with respect to the protein matrix. This leads to the interchange of the two twist angles, τ_{AC} and τ_{BD}, with respect to the protein matrix, making a positive τ_{AC} distribution in isomer A equivalent to a positive τ_{BD} distribution in isomer B. The twist angle distributions point to similar overall heme distortions in both isomers in the protein matrix. This suggests that the macrocycle binds to the protein in a unique conformation, confirming results from the NSD analysis.

The twist angle distributions for the NMR-based trajectories have an inverse relation with those for the crystal-based trajectories. A similar feature was also observed in the NSD analysis, where the ruffling distortions for the NMR- and crystal-based average structures have opposite signs. As indicated earlier, the NMR structures are less well-defined in comparison with the neutron-diffraction structure, and the starting structures for NMR- and crystal-based MD simulations are different. It is possible that the NMR-based trajectories are sampling a conformation space in which the *ruf* deformation has a different value when compared with the crystal-based trajectories. Even in the crystal-based trajectory, the *ruf* deformation can be positive or negative and large for long times (Figure 4a).

Correlation between Rotational Strengths and Heme Distortions. The Soret band of the heme consists of two transitions that are nearly degenerate, polarized in the plane, and at right angles to each other. A planar heme, which is achiral, has zero intrinsic rotational strength. Deviations from planarity introduce chirality in the heme and make the two transitions distinct, resulting in a net intrinsic rotational strength, leading to observable Soret CD. The chiral environment of the protein matrix and the interactions between the chromophores in the protein matrix and the heme can also contribute to Soret CD. The heme structures generated in the MD simulations deviate from planarity and are expected to have intrinsic rotational strength. The intrinsic rotational strength of the heme was calculated by using the PPP approximation and treating the heme π-electron system as a porphyrin dianion.

The heme distortions and the asymmetric substitution pattern break the degeneracy of a planar, 4-fold symmetrical heme. Our initial efforts to correlate the calculated intrinsic rotational strengths of the two Soret transitions with measures of nonplanar distortions, such as ruffling and the average twist angle, were based on classification into high- and low-energy components. This scheme gave double-valued correlations because the near-degeneracy of the Soret components leads to fluctuations in the relative energies of the *x*- and *y*-polarized Soret components and precludes a unique correlation using the energy classification.

Since the two Soret components are polarized perpendicular to each other, the polarization of the two Soret components is more useful for examining correlations. Each Soret transition moment was assigned as either *x*- or *y*-polarized according to the angle of its projection on the mean plane of the heme, using $\pm45°$ lines (the $\alpha-\gamma$ and $\beta-\delta$ axes) as boundaries (Figure 1). Figure 8 shows how the intrinsic rotational strengths of the heme Soret transitions depend on the average twist angle. For both isomers A and B, those transitions polarized predominantly along the *y*-axis have positive rotational strengths for positive τ and negative rotational strengths for negative τ. The rotational strengths of transitions polarized along the *x*-axis show an anticorrelation with τ. There is a substantial scatter, as shown

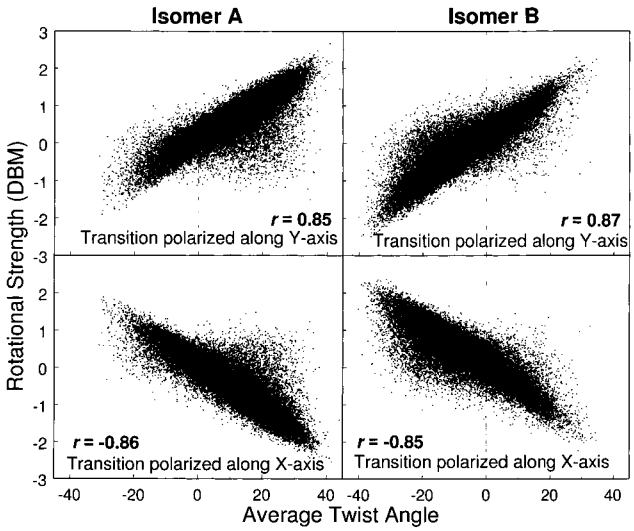

Figure 8. Correlations between average twist angle (τ) and intrinsic rotational strengths of the two Soret components, separated according to their polarization in the heme-plane, for the crystal-based trajectories of isomers A and B.

by the breadth of the distributions, but the correlation coefficients of ca. ± 0.85 indicate that the average twist angle is a good predictor of the sign and approximate magnitude of the intrinsic heme rotational strengths.

As expected from the strong correlation ($r = 0.99$; Figure 6) between the ruffling and the average twist angle, the intrinsic rotational strengths also show a good correlation with the ruffling distortion ($r = \pm 0.86$). Correlation with the other distortion modes (*sad*, *dom*, *pro*, and *wav*) is weak.

Figure 8 shows that isomers A and B give similar correlations between intrinsic Soret rotational strengths and average twist angle. The range of twist angles in isomer B is somewhat larger than that for isomer A, so there are more extreme values of *R*, but the fraction of structures near the extremes is small. For the trajectories shown in Figure 8, there is a bias toward positive twist angles for isomer A, and a more pronounced bias toward negative twist angles for isomer B. As noted previously, these biases have the same net effect but differ in sign because of the 180° rotation about the $\alpha-\gamma$ axis that leads to this interconversion.

In general, the two orthogonally polarized transitions have intrinsic rotational strengths that are opposite in sign, especially at large average twist angles. Thus, the total intrinsic rotational strength is usually small in magnitude compared with the rotational strengths of the individual components. Although the individual components may have $|R| \sim 2$ DBM for twist angles of ca. 20°, the net rotational strengths have maximal magnitudes of ~0.5 DBM. Because of this extensive cancellation and the spread within the individual components, the net intrinsic rotational strength shows no correlation ($r = \pm 0.07$) with the average twist angle and with ruffling. The correlation of total intrinsic rotational strength is shown in Figure 9. The net positive intrinsic rotational strength predicted for both isomers is consistent with the similarity of the heme binding pocket for the two isomers. It must be kept in mind, however, that this similarity may be an artifact resulting from the inadequate starting geometry for isomer B. If a more suitable initial starting geometry can be obtained for isomer B, it is possible that the intrinsic heme rotational strengths for isomer B will be opposite in sign to those for isomer A.

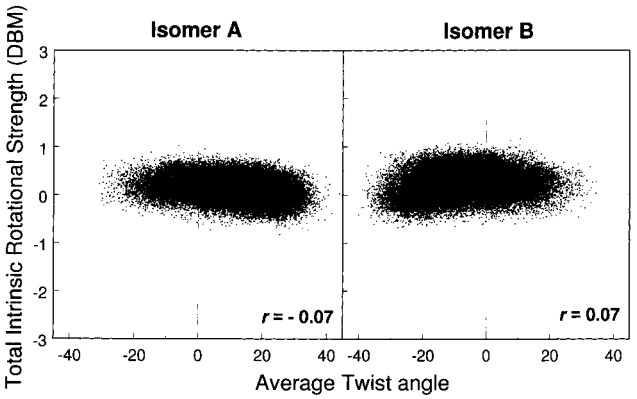

Figure 9. Correlations between average twist angle (τ) and total intrinsic rotational strength for crystal-based trajectories of isomers A and B.

The chromophores of the protein matrix (peptides and aromatic side chains) influence the Soret CD, and they have been included in the calculation of CD of myoglobin according to Tinoco's[28] first-order perturbation approach, as described elsewhere (Kiefl et al., in preparation). The total rotational strength corresponds to the rotational strength of the heme in the protein environment. The total Soret rotational strength in the protein environment shows a weak correlation ($r = \pm 0.40$) with the heme distortions (data not shown). This correlation is mainly due to the influence of the protein environment on heme transitions, since the total intrinsic Soret rotational strength shows no correlation with the heme distortions (Figure 9).

The total Soret CD calculated for the crystal-based MD trajectories of isomer A (Kiefl et al., in preparation) reproduces the strong positive experimental CD spectrum for isomer A of carbonmonoxy myoglobin.[4] The calculated CD based on the trajectories for isomer B (Kiefl et al., in preparation) closely resembles that predicted and observed for isomer A, and therefore does not agree with the weak negative Soret CD band inferred from experiment.[4] The similarity in the spectra predicted for isomers A and B is consistent with the analysis of the heme deformations that indicates qualitatively similar deformations in the two isomers. We suggest that this similarity is an artifact of the method by which the starting structure for simulations of isomer B is prepared. The protein conformations of isomers A and B must be sufficiently different that energy minimization and 600 ps of dynamics at 300 K, following a simple rotation of the heme about the $\alpha-\gamma$ axis, does not overcome a barrier between the two regions of conformational space. Further MD studies are planned using simulated annealing,[29] the coupling parameter method[30] to move smoothly from isomer A to isomer B, or simulation of isomer B in four-dimensional space.[31] The

(28) Tinoco, I., Jr. *Adv. Chem. Phys.* **1962**, *4*, 113−160.
(29) (a) Kirkpatrick, S.; Gelatt, C. D., Jr.; Vecchi, M. P. *Science* **1983**, *220*, 671−680. (b) Brünger, A. T. *Annu. Rev. Phys. Chem.* **1991**, *42*, 197−223.
(30) (a) Berendsen, H. J. C.; Postma, J. P. M.; van Gunsteren, W. F. In *Molecular Dynamics and Protein Structure*; Hermans, J., Ed.; Polycrystal Book Service: P.O. Box 27, Western Springs, IL, 1985; pp 43−46. (b) Jorgensen, W. L.; Ravimohan, C. *J. Chem. Phys.* **1985**, *83*, 3050−3054. (c) Beveridge, D. M.; DiCapua, F. M. *Annu. Rev. Biophys. Biophys. Chem.* **1989**, *18*, 431−492.
(31) (a) van Schaik, R. C.; Berendsen, H. J. C.; Torda, A. E.; van Gunsteren, W. F. *J. Mol. Biol.* **1993**, *234*, 751−762. (b) Beutler, T. C.; van Gunsteren, W. F. *J. Chem. Phys.* **1994**, *101*, 1417−1422.

poorer results obtained for NMR-based trajectories (Kiefl et al., in preparation) are also likely to be the result of inferior starting structures.

Conclusions

The protein maintains the symmetry properties of the heme-binding site even when the heme itself is rotated about the $\alpha-\gamma$ axis. The time-averaged macrocycle structures for isomers A and B largely reflect this site symmetry. This means that the heme in isomer A is distorted in a particular way, but when the heme is rotated by 180°, the same distortion is unfavorable in the binding site and the protein causes the macrocycle conformation to change. For example, doming always occurs in the direction of the proximal ligand, although this appears in the NSD results as a positive doming for isomer A and a negative doming for isomer B.

The 6-ps time average reveals variations in the heme structure at 10- to 100-ps time scales, especially for the softest modes of deformation, saddling and ruffling. Even 600-ps MD trajectories are too short for averaging these motions. Nonetheless, starting from different experimentally obtained initial structures and different initial velocities, generally consistent results were obtained. The original heme distortions of the neutron diffraction structure were qualitatively conserved in the MD trajectories, but long-period variations reflect slow motions of the protein matrix. These slow protein motions show up in the broadening of the Fourier transforms and the very low-frequency components that are present for myoglobin but not for the isolated heme. Examination by NSD of a time series covering an interval of 10 ps shows quasiperiodic variations in the out-of-plane deformations, with ruffling having the largest amplitude and longest period, in accord with the normal-mode analysis of porphyrins.

The average twist angle shows strong correlation with the ruffling deformation and can be used to characterize the overall heme deformation. The intrinsic rotational strengths of the *x*- and *y*-polarized components of the Soret band correlate well with the ruffling deformation and the average twist angle, but not with other types of deformations. The average twist angle can be used to predict the sign and approximate magnitude of the intrinsic heme rotational strengths.

The calculated Soret rotational strengths for the two isomers are positive, and are similar to the experimental value for the equilibrium mixture. The similarity of the rotational strength of the two isomers reflects the similar heme deformations in the protein matrix of both isomers in the simulations. However, this similarity is likely to be caused by a starting structure for isomer B that resembles too closely that for isomer A.

Acknowledgment. The work was supported by National Institute of Health (NIH Grant GM-22994) and the Pittsburgh Supercomputer Center (Grant number MCB980029P). Sandia is a multiprogram laboratory operated by Sandia Corporation, a Lockheed Martin Company, for the United States Department of Energy under Contract DE-AC04-94AL85000.

Supporting Information Available: Details of the MD Simulations; Table S1 (Additions to and Modifications of the GROMOS96 Force Field Parameters); Figure S1 (NSD analysis of heme deformations in164 myoglobin crystal structures), Table S2 (list of 164 structures analyzed in Figure S1), Figures S2−S4 (power spectral density plots of 600-ps trajectories of MbCO isomer A (T2A), MbCO isomer B (T2B), and FePP(Cl) (PDF). This material is available free of charge via the Internet at http://pubs.acs.org.

JA011961W